Chapter 11
Stents: Functions, Characteristics, and Materials

Koichi Tsuchiya and Akiko Yamamoto

Abstract In the last few decades, there has been a remarkable progress in the field of minimally invasive surgery. Such progress has been supported by the invention and development of novel medical devices, such as stents, guide wires, and filters. Stents may be one of the most important devices used for various lesions including coronary, carotid, biliary, etc. Materials used for these devices are divers, ranging from metallic materials (e.g., stainless steels, cobalt-chromium alloys, nitinol, magnesium alloys, etc.) to biodegradable polymers. This chapter introduces the functions of stents and the currently used materials, and also gives some prospect for future materials and device development.

Keywords Stainless steels • Cobalt-chromium alloy • Platinum-chromium alloy • Nitinol • Magnesium alloy

11.1 Introduction

Over the past few decades, minimally invasive surgery has rapidly gained its popularity. Such progress has been supported by the invention and development of novel devices, such as catheters, stents, guide wires, filters, etc. Of particular importance is percutaneous transluminal coronary angioplasty (PTCA) or percutaneous coronary intervention (PCI). As compared to standard open up surgery, PCI has several advantages: minimal physical burden, shorter hospitalized period, fewer number of staffs required for an operation, and lower cost.

The pioneer of the PCI may be Werner Forssmann, who inserted a 65 cm ureteral catheter into a vein of his own arm in 1929. He then walked to X-ray room to film his body and prove that the catheter reached his right ventricle.

K. Tsuchiya (✉)
Research Center for Strategic Materials, National Institute for Materials Science, Sengen 1-2-1, Tsukuba 305-0047, Japan
e-mail: tsuchiya.koichi@nims.go.jp

A. Yamamoto
International Center for Materials Nanoarchitectonics, National Institute for Materials Science, Namiki 1-1, Tsukuba 305-0044, Japan
e-mail: yamamoto.akiko@nims.go.jp

The first PTCA was done by a German cardiologist Andreas Gruentzig. He succeeded to expand the lumens of narrowed arteries by balloon angioplasty in 1977. By 1990, lumen stenosis of the coronary arteries was more commonly treated by the angioplasty technique using a balloon catheter than by standard bypass surgery. But it was also recognized that about 50 % of patients suffered from recurrence of arterial clogging (restenosis) after removal of the balloon. After listening to a talk by Gruentzig in a conference, Julio Palmaz came up with an idea to put a scaffold into a vessel to hold it open and to prevent the restenosis. He co-developed a "stent" with Richard Schatz, and the developed stent was approved for a use in peripheral arteries in 1991 and for coronary in 1994 by the FDA.

After the Palmaz-Schatz stent, numerous types of stents were developed and clinically used in treatment for various lesions. In this chapter, features and characteristics of stents and material aspects of the stents are overviewed.

11.2   Structures and Functions of Stents

A stent is a mesh tube used to prevent the lumen from occlusion (blockage) or stenosis (narrowing) by various disease-induced reasons. An example of a stent and its delivery system is shown in Fig. 11.1. The delivery system is composed of a handle, a catheter, and a sheath, in which a stent is encapsulated. Stents are usually cut out from a metallic tube by precision laser cutting. The diameter of stents is typically 2–5 mm and the length is in the range of 6–30 mm for coronary. For biliary, the diameter is about 6–14 mm and the length 20–150 mm. The stent is composed of struts (frames) and markers, if necessary. Markers are made of radiopaque materials and welded on the both ends of stents.

The stents for the esophagus have a larger dimensions, 16–20 mm diameter, and are woven mesh tubes made of nitinol wires. Grafted stents, or covered stents, are also used for the esophagus.

Stents can be classified into two types depending on how they are deployed: *balloon expandable* and s*elf-expandable*. Balloon-expandable stents are most commonly used for coronary. Procedure of stenting is illustrated in Fig. 11.2. A doctor inserts a catheter through an artery from the groin, leg, or arm. X-ray angiography is used to know the location of the closure and the catheter. Contrast medium, a dye or other substances, is injected into a vein through the catheter near the area of blockage, so the blood flow through the arteries can be visualized on the monitors. The visibility of the stent under X-ray angiography is an important factor for the operation. After placing the stent, the vessel is checked with intravascular ultrasound (IVUS) or by optical coherence tomography (OCT). These devices can image the cross section of the stented vessel and are useful to check the status of the lesion area, e.g., cohesiveness of the stent to the vessel wall.

The design of stent strut varies largely depending on the producer as shown in Fig. 11.3. The complex shape of the stent is designed considering many factors, such as high hoop rigidity, ease of deployment, minimization of recoil,

Fig. 11.1 Stent for the femoral artery (Terumo, "Misago^{TM}", Reprinted from [1] under special permission from Terumo Corporation)
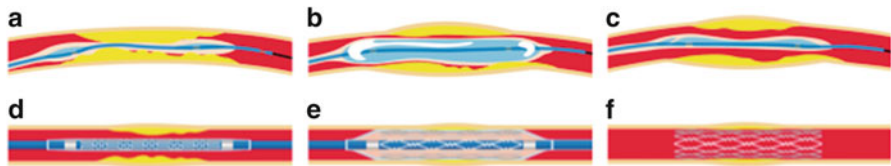

Fig. 11.2 Typical procedure for stenting. (**a**) Balloon catheter is inserted into the vessel to the site of the blockage. (**b**) Balloon is inflated to open the closed vessel. (**c**) Balloon is deflated and balloon catheter is retracted. (**d**) Catheter with a stent and balloon is inserted. (**e**) Balloon is inflated to open the stent. (**f**) Stent keeps the vessel open after the retraction of balloon and catheter

Fig. 11.3 Various designs of stent struts [2]

minimization of axial length change on deployment, uniform application of stress to the vessel wall, flexibility, conformability, and crossability. Stress concentration at both ends of the stent often causes restenosis.

Most of metallic stents are cut from a metallic tube by precision laser cutting. To minimize the internal stress introduced, annealing is applied to improve the fatigue life. In the case of self-expandable stent made of nitinol, shape-setting treatment is applied. Surface finishing of the stents is also very important. Various methods, such as mechanical polishing, blasting, horning, etching, and electropolishing, are used. Most of the stents have markers made of materials with high opacity for X-ray, e.g., platinum, gold, and tantalum, to ensure the visibility of stent position by X-ray angiography. These markers are welded to the struts near the ends of the stents. The possibility of galvanic corrosion has to be taken into consideration.

11.3   Balloon-Expandable Stents

Balloon-expandable stents are manufactured in the diameter that fits in the catheter sheath and expanded to the diameter of the blood vessel by inflating a balloon. Thus, the stents are plastically deformed. Figure 11.4 shows how the hoop stress in stents (lower part of the diagram) and in the vessel (upper part of the diagram) changes on deployment. As it is expanded from the initial diameter (4 mm in the figure), the stents experience the tensile hoop stress up to point b. As the stent touches the vessel of 7 mm diameter at point a, the vessel now experiences the tensile hoop stress which increases to point b. After deflating the balloon, the compressive hoop stress is applied to stents, and the stents recoil to the diameter of 8.25 mm, which corresponds to the diameter at which the stress on the blood vessel and that on the stent balance (point c).

A variety of metallic materials have been used for balloon-expandable stents as summarized in Table 11.1. Most widely used materials for balloon-expandable stents are 316L stainless steel and Co-Cr alloy. SUS316L is the most commonly used metallic material in the biomedical field. The formation of stable Cr_2O_3 passive film leads to better corrosion resistance. The tensile properties can be varied widely by processing conditions.

In the early 2000s, there are a number of reports on the relation between the restenosis and strut thickness of a stent. Several clinical reports [4, 5] indicated that a reduced strut thickness lowers the restenosis rates as shown in Fig. 11.5. These reports drove the demands for stronger and more rigid materials. Co-Cr alloy has a higher strength and better radiopacity than 316L. It also has good corrosion resistance, has good fatigue resistance, and is nonmagnetic. The alloy has been used for medical implants since 1937. The first stent using Co-20Cr-35Ni-10Mo was developed by Medtronic as "Driver[TM]" in 2003. This alloy was originally developed as a heat-resistant alloy known as Elgiloy[TM]. The strut thickness was reduced to 80–90 μm compared to 130–140 μm of earlier SUS316L stents.
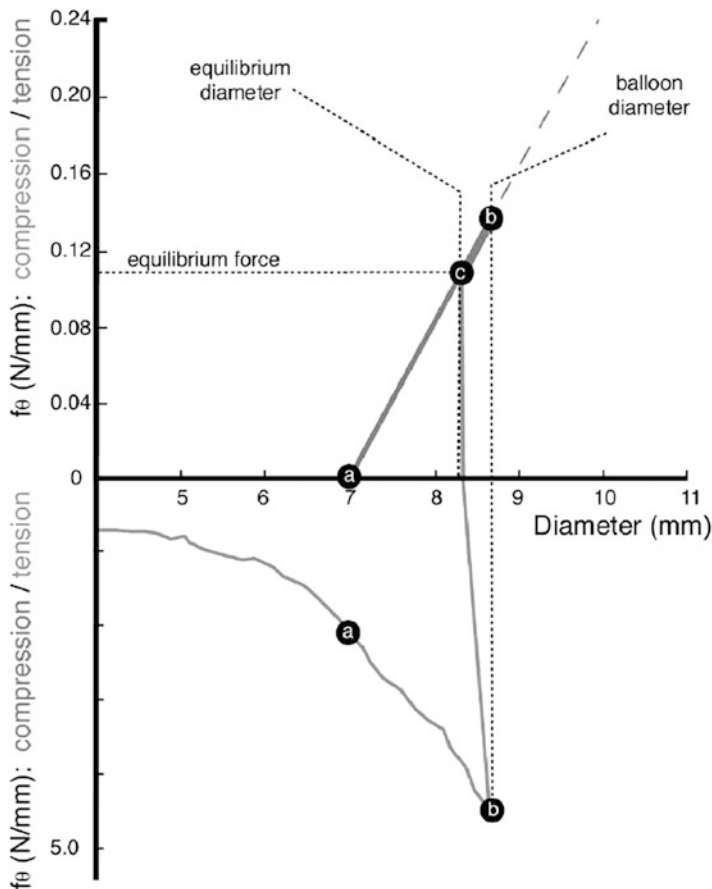
Fig. 11.4 Hoop stress of stent and vessel (Reprinted from [3], Copyright 2002, with permission from Elsevier)

Table 11.1 Metallic materials used for stents

Material	SUS316L	Ta	Co-Cr	Ti	Pt-Cr steels	Nitinol
Young's modulus (GPa)	192	61	200	100–120	191–203	50*
Yield stress (MPa)	175	200	550	310–490	460–480	~200
Tensile stress (MPa)	480	500	720	380–640	824–834	~1,000
Tensile elongation (%)	>40	>60	3	10–20	43.0–44.8	~10
Radiopacity	Normal	Very good	Good	Poor	Very good	Good

Strong demands for materials with a higher strength, rigidity, and radiopacity led to a new alloy specifically designed for coronary stents. Boston Scientific developed Pt-Cr steel, Fe – (32.5–33.5 wt%)Pt – (17.5–18.5 wt%)Cr – (2.43–2.83 wt%) Ni [6, 7]. To attain higher radiopacity, a part of Fe and Ni was substituted by Pt.

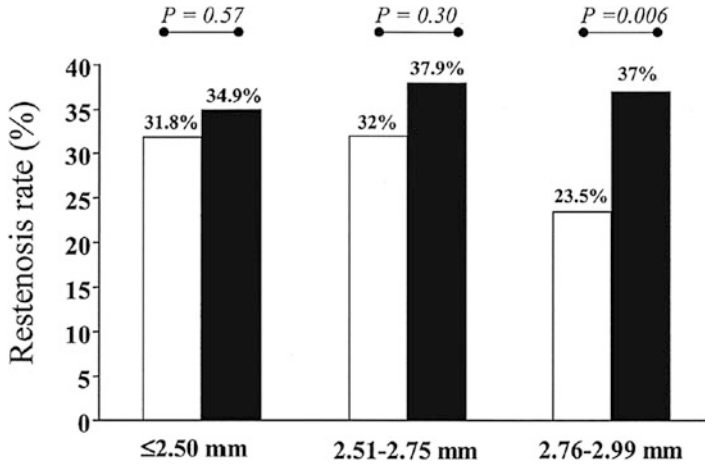**Fig. 11.5** Restenosis rates in lesions treated with a stent with a strut thickness of < 0.10 mm (thin group; open bars) and a stent with a strut thickness ≥ 0.10 mm (thick group; solid bars), according to the reference vessel diameter (≤ 2.50, 2.51–2.75 and 2.76–2.99 mm) (Reprinted from [4], Copyright 2002, with permission from Elsevier)

The amount of Pt was designed to give a good balance between strength, ductility, and radiopacity. The alloy was used for OMEGA^{TM} stents which have a strut thickness of 81 μm and width of 91 μm.

11.4 Self-Expandable Stents

Self-expandable stents are manufactured to be the size of vessel diameter, or slightly larger, and are crimped and constrained in a sheath on a tip of catheter. When it is delivered to the intended site, the sheath is retracted and the stent deploys by itself. Most often, this self-deployment is achieved by superelasticity of shape memory alloy as shown in Fig. 11.6 [8]. Nitinol (TiNi alloy) is almost the only material used for self-expandable stents, due to its superior superelastic properties, good corrosion resistance, and biocompatibility. The basic aspect of nitinol and superelasticity can be found in Chap. 10 or elsewhere [9]. Superelasticity is a kind of pseudoelasticity induced by stress-induced martensitic transformation. As shown in Fig. 11.6, the stress-strain curve is characterized by a stress plateau and large hysteresis. A superelastic stent is in the parent phase when in an unconstrained condition and in the martensite phase when constrained, i.e., inside the sheath. A nitinol stent takes an advantage of the stress plateau and hysteresis. The stents can apply relatively gentle force corresponding to a lower stress plateau to the vessel wall for an extended range of strain. Meanwhile, when an external force is applied to deform or buckle the deployed stent, it resists with the higher stress corresponding to the upper plateau stress. This can be an advantage for the stent
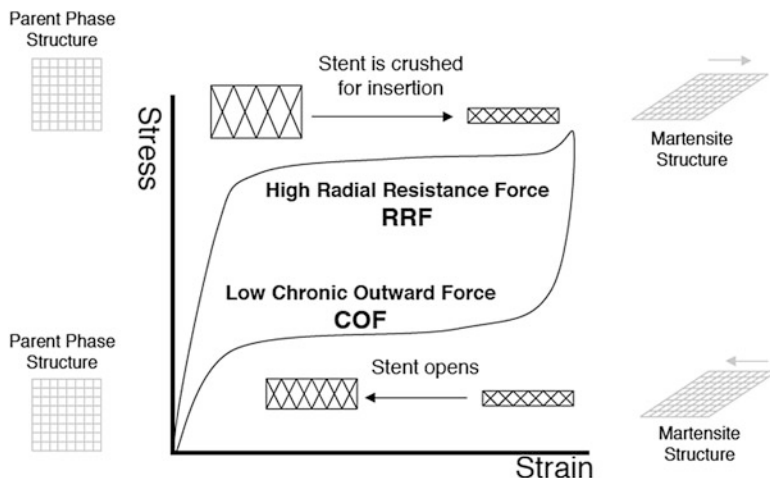
Fig. 11.6 The radial resistive force and chronic outward force as a function of the superelastic hysteresis loop (Reprinted from [8], Copyright 2004, with permission from Elsevier)

which often experiences severe bending or flattering, and thus, the self-expanding stents are most widely used in peripheral as well as biliary arteries. Biliary stents require maneuverability through loops, curvatures, and angulated anatomies and thus high flexibility. A self-expandable stent is also important for carotid and neurovascular vessels since a balloon-expandable stent cannot be used because of a high pressure required for the expansion, which may damage the thin wall of the brain vessels.

11.5   Drug-Eluting Stents (DES)

For bare-metal coronary stents, a clinical report indicated about 20 % of cases ended in restenosis and thrombosis that arise most typically ~30 days after stenting [10]. To minimize this reaction, most of the current coronary stents are drug-eluting stents (DES). The surface of a metallic stent is coated with non-degradable/degradable polymers containing an immunosuppressant or anticancer drug. The first-generation DESs were "Cypher" by Johnson & Johnson and "Taxus" by Boston Scientific. Both used 316L stent as a platform. Most of the second-generation DESs use Co-Cr (Abbott "Xience," Medtronic "Resolute Integrity") or Pt-Cr (Boston Scientific "Promus") stents as the platform. The use of thin strut stents leads to early reendothelialization and is an advantage also for DES [10].

11.6   Bioabsorbable Stents

11.6.1   Emergence of the Research and Development for Bioabsorbable Stents

As described in the previous sections, metallic stents were incorporated into the cardiovascular intervention to give a mechanical support for vessel wall dissections, elastic recoil, and constrictive remodeling of the target lesion after the dilatation of a narrowed artery by a balloon catheter. However, there is still the problem of an in-stent restenosis by neointimal hyperplasia, which is an overgrowth of endothelial and/or smooth muscle cells. The causes of this overgrowth are considered as a physical damage of dilatation, a foreign-body reaction against a metallic stent, and a mechanical stimulation by the stent due to the difference in mechanical properties between the stent and the artery. To solve this problem pharmaceutically, a drug-eluting stent is introduced, which successfully reduced the ratio of in-stent restenosis as between 4 and 15 % [11], but it also caused late and very late stent thrombosis since the stent strut is not covered by the neointima which possibly causes strut malapposition. Therefore, patients should keep taking an antiplatelet drug for a long time such as over a year, which leads to a high risk of hemorrhage and precludes any kind of operation to treat other symptoms. This lack of endothelialization is not observed on the previous bare-metal stents and severely influences the patient's remaining time and quality of life.

As the next generation of cardiovascular intervention, the research and development of bioabsorbable stents, or bioresorbable scaffolds, was started at the end of the twentieth century; the first clinical study of a biodegradable polymer stent was performed in Japan in 1998 [12]. After that, various attempts were made to satisfy the requirement for a bioabsorbable stent, which can dilate the narrowed artery; can support vascular dissections; can prevent elastic recoil, constructive remodeling, and neointimal overgrowth; and, finally, can disappear after a certain period of time, that is, when the physiological remodeling of the target lesion is achieved. The disappearance of the stent will be beneficial not only to avoid the prolonged inflammation at the implanted site causing neointimal hyperplasia but also to enable easy access to the downstream of the artery for another catheter intervention. Another benefit of bioabsorbable stents is the application to infants or children with rapid growth changing the size of organs and blood vessels.

As materials for bioabsorbable stents, not only biodegradable polymers such as poly-L-lactic acids and its copolymers but also metals such as magnesium alloys, iron-based alloys, and pure zinc are now under investigation. Some of them are under clinical studies (see Table 11.2), and no metallic stents but only two types of polymeric stents are available in the market [13]. In the rest of this section, the recent development of these metallic and polymeric stents will be briefly introduced.

Table 11.2 Clinical results of bioabsorbable stents [13, 43]

Name	Material	Drug elution	Total strut thickness (μm)[a]	Stent coverage (%)	LLL at 6 months (mm)	TLR rate at 1 year (%)
AMS®-1	WE43	−	165	10	1.08 ± 0.49 (at 4 months)	45 %
DREAMS®1	WE43	+	125		0.64 ± 0.50	9.1 % (at 6 months)
Igaki-Tamai®	PLLA	−	170	24	0.91 ± 0.69	
Absorb®1.0	PLLA	−	156	25	0.43 ± 0.37	0 %
Absorb®1.1	PLLA	+	156	25	0.19 ± 0.18	3.6 %
REVA®	Polymer[b]	−	200	55	1.46 ± 0.71	67 %
DESolve®	Polymer[c]	+	200	65	0.21 ± 0.34 or 0.19 ± 0.19[d]	

[a]Including coating
[b]Poly-tyrosine-derived polycarbonate
[c]Salicylate-derived polymer
[d]Two types of drugs are coated separately

11.6.2 Magnesium Alloy

Magnesium and its alloys are one of the candidates for bioabsorbable metals since magnesium is easily corroded by reacting with water in the body fluid. Furthermore, magnesium is an essential element for the human being, and its concentration in an adult human is the fourth highest among all metallic elements, following sodium, potassium, and calcium. Therefore, the acceptable upper limit of released ion concentration is expected to be high, suggesting low possibility of toxic reaction due to the released Mg^{2+} ions. Because of its high specific strength and Young's modulus, which is closer to that of human cortical bone, Mg alloys first applied to the orthopedic field. In 2003, however, a first magnesium stent made with AE21 (Mg-2wt.%Al-1wt.%RE, RE: mixture of rare earth element) was implanted into a porcine artery, and its endothelialization was confirmed at day 35 [14]. Further investigation with swine or minipig models revealed less neointimal formation of magnesium alloy stents made with WE43(Mg-4wt%Y-3wt%RE)-based alloy than that of 316L stainless steel bare-metal stents [15, 16]. After 3 months of implantation into swine arteries, the disappearance of the WE43-based alloy stent was confirmed (see Fig. 11.7) [17]. A preclinical study of AZ31(Mg-3wt.%Al-1wt.% Zn) alloy stent was also performed with rabbit aorta model, reporting that the non-polymer-coated, phosphorized AZ31 stent disappeared around 105 days[18].

Several clinical studies were already reported for the WE43-based alloy stent. At the first clinical study performed in 2004, 23 stents were implanted into the ischemic lower limb of 20 patients [19–21], reporting no acute toxic reaction due to the magnesium stent implantation, and the stents degraded within 6 weeks [19–21]. The safety of the WE43-based stent was also confirmed by the clinical cases with preterm and newborn infants [22, 23]. Further investigation to the coronary arteries was carried out for 63 patients with 71 stents and resulted in 45 % of target lesion revascularization (TLR) at 12 months after operation, which is higher than those of current bare-metal stents (28 %) or DES (6 %) [24]. The implanted WE43-based stents were considered to be degraded within 4 months [24]. These studies suggested the lack of the duration maintaining stent integrity; in other words, the degradation rate of employed stents is too fast for this application. Supposing the cross section of a stent strut as 150×150 μm^2 and the degradation period as 1 year, the estimated corrosion rate is about 75 μm/year. This is not the easy value to achieve by conventional magnesium alloys. These clinical studies also revealed lower risk of late thrombosis which is an issue for recent drug-eluting stents.

Aiming to improve the duration of maintaining mechanical integrity at the coronary artery and to reduce the ratio of the patients with revascularization, a polymer-coating drug-eluting WE43-based stent is prepared and investigated with a porcine coronary model. In this study, the degradation rate of the stent after 28 days of implantation is 0.036–0.072 mg/cm$^2 \cdot$d (=72–144 μm/year) and the stent disappeared within 6 months [25]. The clinical study of this drug-eluting magnesium stent found that the late lumen loss (LLL) at 12 months postoperation successfully reduced to 0.52 ± 0.39 mm from 1.08 ± 0.49 mm of the non-coated
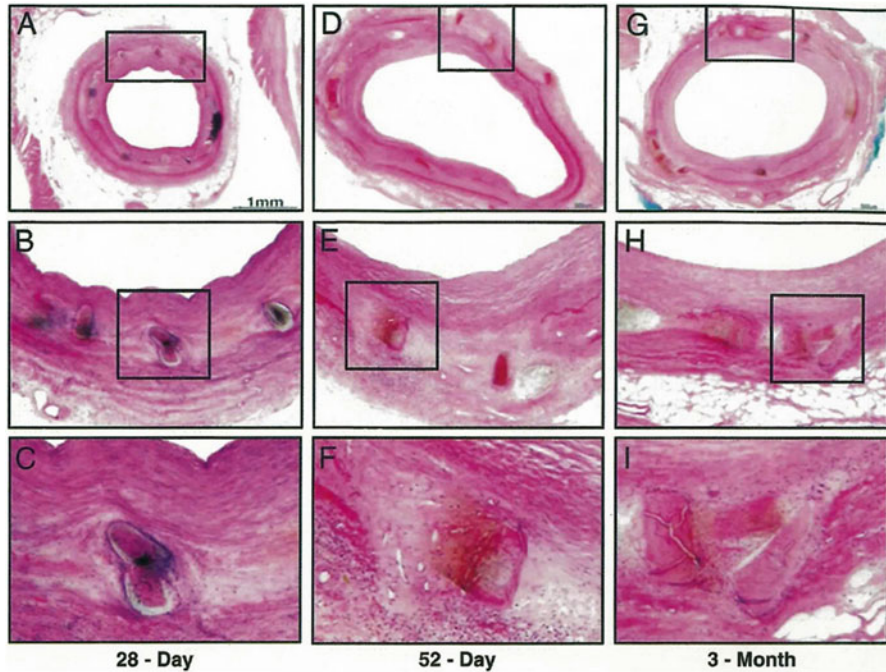
Fig. 11.7 Histology of porcine coronary arteries implanted with WE43-based stents (AMS-1) for 28 days (A, B, C), 52 days (D, E, F), and 3 months (G, H, I) (Reprinted from Ref. [17], Copyright 2008 with permission from Elsevier)

magnesium stent [26, 27]. However, this value is not close to that of a biodegradable polymer stent, Absorb1.1, that is, 0.27 ± 0.32 mm at 12 months postoperation [13]. Therefore, modification of WE43-based magnesium drug-eluting stent is attempted on the following points: increasing the strut thickness to 150 μm, attaching tantalum radiopaque markers at both ends, increasing the number of strut crowns per stent length, changing the drug and the biodegradable polymer, and increasing the coating thickness (see Fig. 11.8) [27]. This new version of biodegradable WE43-based magnesium stent is now under clinical study as the BIOSOLVE-II trial.

To satisfy the requirement in the degradation rate of magnesium alloy stents, development of new magnesium alloys, microstructure controlling processes, and coating/surface modification technologies are carried out by various research groups, which are well described in other review articles [28–30]. Most of these researches are still at a laboratory level, not at clinical nor preclinical level yet.

Since magnesium alloys generally take a hexagonal closed-packed system having a few slip planes available at room temperature, plastic working of magnesium alloys requires heating around 573 K ($=300\ °C$). The melting point of pure magnesium is relatively low at 923 K ($=650\ °C$), suggesting heating susceptibility of the microstructure. A laser cutting process of a stent strut from a thin tube may
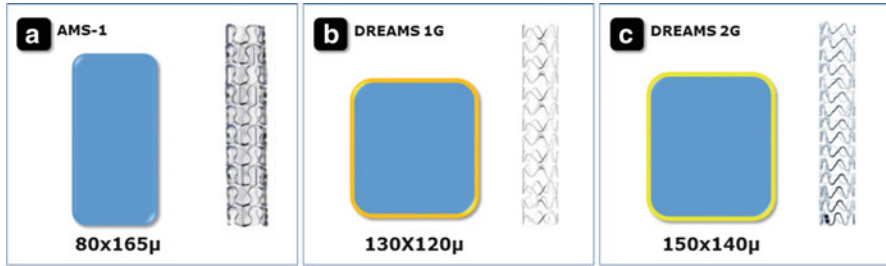
Fig. 11.8 Schematic cross-sectional profiles of WE43-based stent struts of AMS-1 (**a**), drug-eluting absorbable metal scaffold, DREAMS 1st generation (**b**), and DREAMS 2nd generation (**c**). The poly(lactide-co-glycolide) coating with paclitaxel is shown as a thin orange layer in (**b**), whereas the polylactide coating with sirolimus is shown in thin yellow layer in (**c**) [27]

locally influence alloy microstructure. Technological development of fabrication processes is also important for the success of magnesium alloy stents.

11.6.3 Iron and Its alloy

Iron is another candidate for bioabsorbable metals since it is an essential element for the human being, expecting relatively low toxicity, and it also has relatively low corrosion resistance in the biological environment. Because of the relatively low mechanical properties and too fast degradation of magnesium alloys, stent application of pure iron and iron-based alloys attracted several groups of researchers, but no clinical study is reported yet.

First preclinical investigation of pure iron stent was carried out by a rabbit aorta model in 2001 [31], followed by a porcine artery model [32, 33]. At 18 months postoperation in a rabbit model, the exact degradation rate of iron stent was too difficult to assess even though brownish corrosion products were observed surrounding the stent strut with macrophages as a sign of mild local inflammation [31]. The colorization of the tissue surrounding stent struts was also observed in porcine cases, starting at 14 days of implantation and longer (see Fig. 11.9) [32, 33]. The excretion of the corrosion products by the reticuloendothelial system was observed after 1 month postoperation, showing small amounts of macrophages containing corrosion products in the lymph nodes near the implantation site [33]. After 3-month implantation, focal accumulation of the corrosion products was observed in the spleen, as well as macrophages containing irons in the lymphatic pathways along the aorta [33]. However, no sign of significant iron overload was reported [31, 33], since the implanted amount of iron is small as several tens of micrograms, which is much lower than the overload level for a whole animal.

Stent integrity was maintained to the end of the follow-up period as it was hardly degraded during 12–18 months [31, 33]. Complete endothelialization was
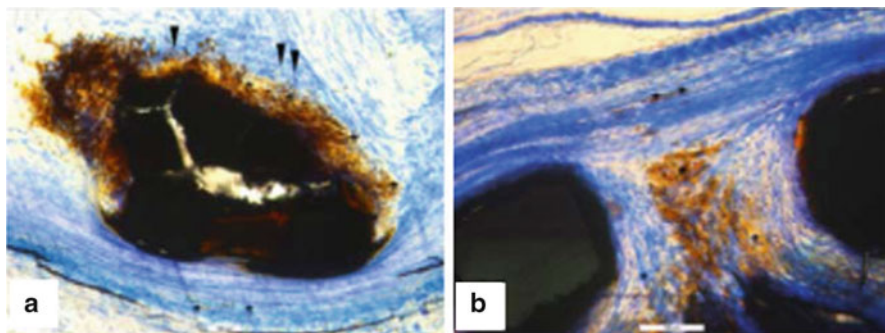
Fig. 11.9 Histology of iron stent struts after implantation of 180 (**a**) and 360 (**b**) days into porcine aorta (Reprinted from Ref. [33], Copyright 2006, with permission from Elsevier)

observed, resulting in no obvious thrombogenesis [31–33]. The angiographic results revealed no significant difference between the 316L and Co-Cr alloy control stents [31–33]. These studies suggests that the excretion of corrosion products around the struts may cause a local, prolonged inflammation even though the amount of corrosion products is very low to cause any overdose reaction at a specific organ. It is also suggested that the degradation rate of pure iron stent is too low for a coronary stent, which is ideal to disappear in 12–24 months after implantation even though there is still a discussion about an optimal degradation period and mechanical integrity duration among researchers [29].

To shorten the degradation period of the iron stent, vacuum plasma nitriding was employed to prepare a stent with thinner (70 μm) strut [34]. Implantation into mini-pig up to 28 days reported no significant difference in the endothelialization ratio, vascular histomorphometry, and other histological observations [34] as similar to the previous in vivo studies. However, no information about the degradation of the iron stent was reported due to the short (28 days) follow-up period.

Other approaches to reduce the degradation period of iron stent are microstructure control such as equal channel angular pressure (ECAP) technique [35] or electroforming [36] and alloying. Fe-Mn alloys are mainly investigated [37–39].

11.6.4 Zinc

To achieve an ideal degradation rate for a bioabsorbable coronary stent that is lower than magnesium alloys but higher than pure iron, application of pure zinc is attempted. Zinc is also an essential element for the human being, but the concentration of zinc in the human blood plasma is 12–18 μM (=0.8–1.2 mg/L), which is much smaller than that of magnesium (0.5–1 mM = 12–24 mg/L) [40]. The concentration of zinc in blood plasma of a patient with zinc overdose symptom is reported as 31.5–640 μM (=2.1–42 mg/L), whose lower value is much smaller than

that of magnesium as > 2.5 mM (>60.8 mg/L) as well [41]. These data indicate that the acceptable range of the zinc concentration in blood plasma is not so wide, suggesting that the implantation of zinc as a larger device is probably not recommended. Since a coronary stent prepared from pure zinc probably has a weight of only around 50 mg, an assumption of degrading by 12 months gives the daily release about 0.14 mg/day, which is below the plasma concentration in the overdose case.

An in vivo study implanting a pure zinc wire into a rat abdominal aorta reported that the initial degradation rate at 1.5 months was less than 20 μm/year [42]. After 4 months of implantation, the cross-sectional area of the implanted wire reduced to about 70 % of that of the initial condition, with no obvious sign of tissue necrosis or repulsion [42]. However, the tensile strength of pure zinc is ∼ 120 MPa [42], suggesting the necessity of alloying and microstructure modification to improve the mechanical properties while maintaining its "favorable" degradation rate.

11.6.5 Biodegradable Polymers

To date, the most successful bioabsorbable stent is prepared with semi-crystalline poly-L-lactic acid (PLLA) coated with poly(D,L-lactic acid) containing an antiproliferative drug (everolimus) [13]. The stent design is in-phase hoops with straight links to each other with platinum markers, maintaining radial support for 6 months and disappearing within 2 years [33]. Clinical studies of the latest version of this stent reported LLL at 6 and 12 months postoperation as 0.19 ± 0.18 mm and 0.27 ± 0.32 mm, respectively [13]. Other clinical parameters such as TLR rate are also comparable to those of the latest, most popular drug-eluting stents [13]. However, the lower mechanical properties of bioabsorbable polymer stents than those of conventional metallic stents restrict their stent design, especially strut thickness, and thus reduce their deliverability and applicable clinical conditions. Therefore, clinical studies in a larger scale and wider application are in progress as the ABSORB II and the ABSORB EXTEND, as well as worldwide evaluation programs in Asia, Africa, and Australia.

Another stent available in the market has a similar structure, a PLLA-based stent containing two novel antiproliferative drugs (Novolimus and Myolimus), designed to have out-of-phase hoops with straight links and to disappear within 2–3 years [13]. Small-scale clinical studies also reported LLL at 6 months as 0.19 ± 0.19 mm for Novolimus and 0.21 ± 0.34 mm for Myolimus [13]. The endothelialization ratio at 6 months is 98.7 ∼ 98.8 % for both drugs [13].

Among several developments of a polymer-based bioabsorbable stent in progress, a few have unique strategies to conquer some drawbacks of PLLA-based bioabsorbable stents. One of them employs poly-tyrosine-derived polycarbonate polymer containing iodine to be radiopaque with a tubular "slide-and-lock" design [43]. Another uses poly(anhydride-ester) based on salicylic acid and adipic acid anhydride, having a tubular design with laser-cut voids [13]. The features of these

stent designs are relatively high coverage of artery as 55–65 %, whereas those of conventional metallic stents and successful PLLA ones are about 10 % and 25 %, respectively [33]. This high coverage enables to increase the mechanical integrity and drug dose, as well as to reduce dissected area of artery and penetration of loose plaque. However, small-scale clinical studies for these stents resulted in high TLR rate at 12 months of about 67 % for the poly-tyrosine-based stent [43] or increased neointimal formation for the poly-salicylate-based stent [13], forcing redesigning of both stents.

11.7 Summary and Perspective

In this chapter, functions and characteristics of stents and materials used for the stents were overviewed. The current status of research and development on biodegradable stents, the next generation of vascular intervention, was also reviewed. A key issue for the success of metal-based bioabsorbable stents is to achieve a clinical result comparable to the polymer-based stents with a similar level of mechanical support to conventional metallic stents. The trend of miniaturization of the stents, i.e., thinner struts, smaller area, and smaller diameter in a crimped state, will continue in the future since it is beneficial for faster remodeling of vessel walls and better maneuverability on delivery. This trend requires materials with even higher strength, higher rigidity, and higher radiopacity. One possible method to achieve higher strength may be microstructure refinement by severe plastic deformation. There are extensive researches going on about this subject, and a number of results were reported in the application to artificial joints or orthodontic wires, but applications to vascular indwelling devices are scarcely seen [44]. Ultrafine grains or nanograins may also be beneficial to improve the corrosion resistance. Microstructure control can influence cellular response to metal surface via protein adsorption behavior [45, 46]. Rigidity or elastic modulus as well as radioopacity is an "element-dependent" property, and it is difficult to control by microstructures. One interesting exemption is nitinol, in which nanograins or even amorphous phase can be easily obtained by plastic deformation. Increase in Young's modulus was reported in severely cold-drawn wires [47] or SMAT (surface mechanical attrition)-treated samples [48]. But this is a special case; composite or hybrid materials approach may be necessary to obtain high-modulus materials.

References

1. http://www.terumo.co.jp/medical/equipment/me240.html
2. Baskot BG (ed) (2013) What should we know about prevented, diagnostic, and interventional therapy in coronary artery disease. Intech (Open access book available at http://www.intechopen.com/books/)

3. Duerig TW, Wholey MA (2002) Comparison of balloon- and self-expanding stents. Minim Invas Ther Allied Technol 11:173–178
4. Briguori C, Sarais C, PagnottaP LF, Montorfano M, Chieffo A, Sgura F, Corvaja N, Albiero R, Stankovic G, Toutoutzas C, Bonizzoni E, Di Mario C, Colombo A (2002) In-stent restenosis in small coronary arteries. J Am Coll Cardiol 40:403–409
5. Pache J, Kastrati A, Mehilli J, Schuhlen H, Dotzer F, Hausleiter J, Fleckenstein M, Neumann F-J, Sattelberger U, Schmitt C, Muller M, Dirschinger J, Shomig A (2003) Intracoronary stenting and angiographic results: strut thickness effect on restenosis outcome (ISAR-STEREO-2) trial. J Am Coll Cardiol 41:1283–1288
6. O'Brien BJ, Stinson JS, Larsen SR, Eppihimer MJ, Carroll WM (2010) A platinum-chromium steel for cardiovascular stents. Biomaterials 31:3755–3761
7. Allocco DJ, Jacoski MV, Huibregste B, Mickley T, Dawkins KD (2011) Platinum chromium stent series. Interv Cardiol 6:134–141
8. Morgan NB (2004) Medical shape memory alloy applications – the market and its products. Mater Sci Eng A378:16–23
9. Yamauchi K, Ohkata I, Tsuchiya K, Miyazaki S (2011) Shape memory and superelastic alloys. Woodhead Publishing, Cambridge
10. Suzuki T (2014) Present and future requirements for materials in cardiovascular intervention. Materia Jpn 53:148–152
11. Erne P, Svhirt M, Resink TJ (2006) The road to bioabsorbable stents: reaching clinical reality? Cardiovasc Interv Radiol 29:11–16
12. Tamai H, Igaki K, Kyo E, Kosuga K, Kawashima A, Matsui S, Komori H, Tsuji T, Motohara S, Uehata H (2000) Initial and 6-month results of biodegradable poly-l-lactic acid coronary stents in humans. Circulation 102:399–404
13. Campos CAM, Zhang YJ, Bourantas CV, Muramatsu T, Garcia-Garcia HM, Lemos PA, Iqbal J, Onuma Y, Serruys PW (2013) Bioresorbable vascular scaffolds in the clinical setting. Interv Cardiol 5:639–646
14. Heublein B, Rohde R, Kaese V, Niemeyer M, Hartung W, Haverich A (2003) Biocorrosion of magnesium alloys: a new principle in cardiovascular implant technology? Heart 89:651–656
15. Waksman R, Pakala R, Kuchulakanti PK, Baffour R, Hellinga D, Seabron R, Tio FO, Wittchow E, Hartwig S, Harder C, Rohde R, Heublein B, Andreae A, Waldmann KH, Haverich A (2006) Safety and efficacy of bioabsorbable magnesium alloy stents in porcine coronary arteries. Catheter Cardiovasc Interv 68:607–617
16. Loos A, Rohde R, Haverich A, Barlach S (2007) In vitro and in vivo biocompatibility testing of absorbable metal stents. Macromol Symp 253:103–108
17. Slottow TLP, Pakala R, Okabe T, Hellinga D, Lovec RJ, Tio FO, Bui AB, Waksman R (2008) Optical coherence tomography and intravascular ultrasound imaging of bioabsorbable magnesium stent degradation in porcine coronary arteries. Cardiovasc Revasc Med 9:248–254
18. Li H, Zhong H, Xu K, Yang K, Liu J, Zhang B, Zheng F, Xia Y, Tan L, Hong D (2011) Enhanced efficacy of sirolimus-eluting bioabsorbable magnesium alloy stents in the prevention of restenosis. J Endovasc Ther 18:407–415
19. Mario H, Griffiths CD, Goktekin O, Peeters N, Verbist J, Bosiers M, Deloose K, Heublein B, Rohde R, Kasese V, Ilsley C, Erbel R (2004) Drug-eluting bioabsorbable magnesium stent. J Interv Cardiol 17:391–395
20. Peeters P, Bosiers M, Verbis J, Deloose K, Heublein B (2005) Preliminary results after application of absorbable metal stents in patients with critical limb ischemia. J Endovasc Ther 12:1–5
21. Bosiers M, Deloose K, Verbist J, Peeters P (2006) Will absorbable metal stent technology change our practice? J Cardiovasc Surg 47:393–397
22. Zartner P, Cesnjevar R, Singer H, Weyand M (2005) First successful implantation of a biodegradable metal stent into the left pulmonary artery of a preterm baby. Catheter Cardiovasc Interv 66:590–594

23. Schranz D, Zartner P, Michel-Behnke I, Akintürk H (2006) Bioabsorbable metal stents for percutaneous treatment of critical recoarctation of the aorta in a newborn. Catheter Cardiovasc Interv 67:671–673
24. Erbel R, Mario CD, Bartunek J, Bonnier J, de Bruyne B, Eberli FR, Erne P, Haude M, Heublein B, Horrigan M, Ilsley C, Böse D, Koolen J, Lüscher TF, Weissman N, Waksman R (2007) Temporary scaffolding of coronary arteries with bioabsorbable magnesium stents: a prospective, non-randomized multicentre trial. Lancet 369:1869–1875
25. Wittchow E, Adden N, Riedmüller J, Savard C, Waksman R, Braune M (2013) Bioresorbable drug-eluting magnesium alloy scaffold: design and feasibility in a porcine coronary model. Eurointervention 8:1441–1450
26. Haude M, Erbel R, Erne P, Verheye S, Degen H, Böse D, Vermeersch P, Wijnbergen I, Weissman N, Prati F, Waksman R, Koolen J (2013) Safety and performance of the drug-eluting absorbable metal scaffold (DREAMS) in patients with de-novo coronary lesions: 12 month results of the prospective, multicentre, fist-in-man BIOSOLVE-I trial. Lancet 381:836–844
27. Campos CM, Muramatsu T, Iqbal J, Zhang YJ, Onuma Y, Garcia-Garcia HM, Haude M, Lemos PA, Warnack B, Serruys PW (2013) Bioresorbable drug-eluting magnesium-alloy scaffold for treatment of coronary artery disease. Int J Mol Sci 14:24492–24500
28. Li N, Zheng Y (2013) Novel magnesium alloys developed for biomedical application: a review. J Mater Sci Technol 29:489–502
29. Moravej M, Mantovani D (2011) Biodegradable metals for cardiovascular stent application: interests and new opportunities. Int J Mol Sci 12:4250–4270
30. Wang J, Tang J, Zhang P, Li Y, Wang J, Lai Y, Qin L (2012) Surface modification of magnesium alloys developed for bioabsorbable orthopedic implants: a general review. J Biomed Mater Res 100B:1691–1701
31. Peuster M, Wohlsein P, Brügmann M, Ehlerding M, Seidler K, Fink C, Brauer H, Fischer A, Hausdorf G (2001) A novel approach to temporary stenting: degradable cardiovascular stents produced from corrodible metal–results 6–18 months after implantation into New Zealand white rabbits. Heart 86:563–569
32. Waskman R, Pakala R, Baffour R, Seabron R, Hellinga D, Tio FO (2008) Short-term effect of biocorrodible iron stents in porcine coronary arteries. J Interv Cardiol 21:15–20
33. Peuster M, Hesse C, Schloo T, Fink C, Beerbaum P, von Schnakenburg C (2006) Long-term biocompatibility of a corrodible peripheral iron stent in the porcine descending aorta. Biomaterials 27:4955–4962
34. Wu C, Qiu H, Hu X, Ruan Y, Tian Y, Chu Y, Xu X, Xu L, Tang Y, Gao R (2013) Short-term safety and efficacy of the biodegradable ion stent in mini-swine coronary arteries. Chin Med J 126:4752–4757
35. Nie F, Zheng Y, Wei S, Hu C, Yang G (2010) In vitro corrosion, cytotoxicity and hemocompatibility of bulk nanocrystalline pure iron. Biomed Mater 5:065015
36. Moravej M, Purnama A, Fiset M, Couet J, Mantovani D (2010) Electroformed pure iron as a new biomaterial for degradable stents: in vitro degradation and preliminary cell viability studies. Acta Biomater 6:1843–1851
37. Hermawan H, Dube D, Mantovani D (2010) Degradable metallic biomaterials: design and development of Fe-Mn alloys for stents. J Biomed Mater Res 93A:1–11
38. Schinhammer M, Hanzi AC, Loffler JF, Uggowitzer PJ (2010) Design strategy for biodegradable Fe-based alloys for medical applications. Acta Biomater 6:1705–1713
39. Liu B, Zheng Y, Ruan L (2010) In vitro investigation of Fe30Mn6Si shape memory alloy as potential biodegradable metallic material. Mater Lett 65:504–543
40. Haraguchi H (2005) Seimei to kinzoku no sekai (The world of life and metals), Foundation for the Promotion of the Open University of Japan, Tokyo, p 273 (in Japanese)
41. Suzuki T, Wada O (eds) (1994) Mineral, biryo-genso no eiyougaku (Nutritional Science of minerals and trace elements). Dai-ichi shuppan, Tokyo

42. Bowen PK, Drelich J, Goldman J (2013) Zinc exhibits ideal physiological corrosion behavior for bioabsorbable stents. Adv Mater 25:2577–2582
43. Serruys PW, Garcia-Garcia HM, Onuma Y (2012) From metallic cages to transient bioresorbable scaffolds: change in paradigm of coronary revascularization in the upcoming decade? Eur Heart J 33:16–25
44. Ge Q, Dellasega D, Demir AG, Vedani M (2013) The procession of ultrafine-grained Mg tubes for biodegradable stents. Acta Biomater 9:8604–8610
45. Shri DNA, Tsuchiya K, Yamamoto A (2014) Effect of high-pressure torsion deformation on surface properties and biocompatibility of Ti-50.0 mol.%Ni alloys. Biointerphases 9:029007
46. Shri DNA, Tsuchiya K, Yamamoto A (2014) Cytocompatibility evaluation and surface characterization of TiNi deformed by high-pressure torsion. Mater Sci Eng C 43(2014):411–417
47. Tsuchiya K, Hada Y, Ohnuma M, Namajima K, Koike T, Todaka Y, Umemoto M (2009) Production of TiNi amorphous/nanocrystalline wires with high strength and elastic modulus by severe cold drawing. Scr Mater 60:749–752
48. Mei QS, Zhang L, Tsuchiya K, Gao H, Ohmura T, Tsuzaki K (2010) Grain size dependence of elastic modulus in nanostructured NiTi. Scr Mater 63:977–980